TECHNICAL NOTE

TECHNICAL NOTE 78.92

Biofilm studies in compartment III pilot reactor: Analysis and discussion of the results

Prepared by/Préparé par	Anna Montràs, Larissa Hendrickx, Julio Pérez
Reference/Réference	CCN7 to contract 13292/98/NL/MV
Issue/Edition	1
Revision/Révision	0
Date of issue/Date d'édition	15/02/08
Status/Statut	Final

TECHNICAL NOTE

APPROVAL

Title *Titre*	Biofilm studies in compartment III pilot reactor: Analysis and discussion of the results	Issue *Edition*	1	Revision *Révision*	0

Author *Auteur*	Anna Montràs, Larissa Hendrickx, Julio Pérez	Date *Date*	15/02/08

Approved by *Approuvé par*	Brigitte Lamaze	Date *Date*	15/02/08

CHANGE LOG

Issue/*Edition*	Revision/*Révision*	Status/*Statut*	Date/*Date*

Distribution List

Name/*Nom*	Company/*Société*	Quantity/*Quantité*

TABLE OF CONTENT

1. INTRODUCTION 4
2. QUANTIFICATION OF CLSM IMAGES 5
3. PRESENCE OF EXTRACELLULAR POLYMERIC SUBSTANCES (EPS) IN THE BIOFILM 9
4. BIOMASS CONCENTRATION PROFILE 12
5. RELATIVE DISTRIBUTION OF *N. europaea* AND *N. winogradskyi* ALONG THE PACKED-BED 14
6. CONCLUSIONS 20
7. LIST OF ABBREVIATIONS AND ACRONYMS 21
8. REFERENCES 21
9. ANNEX 26
10. COMMENTS 27

1. INTRODUCTION

The goal of nitrification in the MELiSSA loop is the oxidation of the ammonia present in the organic waste to nitrate, in order to provide a more suitable source for compartment IV. The strains selected to perform nitrification in the MELiSSA are *Nitrosomonas europaea* ATCC 19718 and *Nitrobacter winogradskyi* ATCC 25391, which perform the oxidation of ammonia to nitrite and nitrite to nitrate respectively.

Due to the low growth rate nitrifiers require, immobilization of the co-culture on a substrate is necessary. In addition, a nitrifying biofilm will provide for the most appropriate biochemical engineering strategy, when treating the high nitrogen loads that will be present in the organic waste. Hence, an upflow cocurrent packed-bed bioreactor was used to achieve the biological oxidation of ammonia to nitrate (Gòdia *et al.*, 2002)

The factors contributing to the hydrodynamics of a packed-bed biofilm reactor were previously studied in order to characterize the liquid phase mixing. Residence Time Distribution (RTD) analysis performed in this reactor indicated a very close to perfectly mixed tank behaviour for the liquid phase, with only a small percentage of plug-flow (Pérez *et al*., 2004). Nevertheless, this small deviation was causing a gradient of biofilm thickness along the packed-bed due to the difference between the characteristic times of nitrification and mixing (Pérez et al., 2004).

A mathematical model was used to describe the efficiency of nitrification in the packed-bed (Pérez et al., 2005). This model did not include diffusion of substrates into the biofilm. However, even with this simplified approach the results obtained with that model pointed at a possible segregation of *N. europaea* and *N. winogradskyi* along the packed-bed vertical axis.

Several authors have observed a segregation of Ammonia Oxidizing Bacteria (AOB) and Nitrite Oxidizing Bacteria (NOB) in biofilm populations of artificial waste treatment systems, both on the microscopical (Schramm et al., 2000; Schramm, 2003; Okabe *et al.*, 1999) and on the macroscopical scale (Noto *et al*., 1998; Holben *et al.*, 1998; Lydmark *et*

al., 2006). To investigate nitrifyers in biofilm systems, Fluorescent *In Situ* Hybridization (FISH) (Schramm et al., 2000; Lydmark *et al.*, 2006), 16S ribosomal DNA cloning analysis (Okabe et al., 2002) or real-time quantitative polymerase chain reaction (RTQ-PCR) (Kindaichi et al., 2006) were applied.

In the present study, FISH was used on samples obtained from different heights along the fixed bed, in order to assess the relative distributions of *N. europaea* and *N. winogradskyi*. The use of FISH coupled with Confocal Laser Scanning Microscopy (CLSM) to study bacterial distribution in biofilms has been well reported in the literature and offered all the necessary probes and hybridisation conditions needed to perform the study described in this report (Thurnheer et al., 2004; Persson et al., 2002; Nogueira et al., 2002; Sakano et al., 2002).

In technical note 78.91 an extensive description of all the techniques and protocols used for the study of the biofilm in compartment III upon stop of its operation was provided. An outline of the general trends, along with some qualitative results, was also presented in order to illustrate the extent of the biofilm studies performed in compartment III. A full report of the results obtained from the biofilm studies will be provided in the present technical note.

2. QUANTIFICATION OF CLSM IMAGES

A LEICA DM IRE2 inverted CLSM (LEICA Microsystems, Germany) was used for image acquisition. The microscope was fitted with a TCS SP2 AOBS confocal laser scanning system. As described in TN 78.91, the different r-RNA probes that target cells with certain specificity are tagged with different fluorochromes that can be visualized with a fluorescence microscope. In this case the use of a CLSM makes it possible not only to detect and visualize the different fluorochromes, but also to obtain images at different depths of the sample, making it possible to obtain a series of images along the z-axis of the biofilm in 10 µm section intervals.

The 256 gray-scale-level images obtained with the CLSM (Fig. 1A) for each fluorochrome were converted into binary images by manually selecting a threshold level using the Leica Confocal Software (Leica, Heidelberg, Germany) as the tool for image analysis. Thresholds were manually selected in order to enhance the accuracy in the quantification process (Yang et al., 2001), with the lowest intensity for each channel selected as the threshold value. Although automatic thresholding methods would provide higher reproducibility than manual thresholding, better accuracy is obtained by using manual thresholding.

Thresholding was achieved by defining an intensity below which any pixel was assigned an intensity of 0 while the pixels above the threshold were assigned 256 and thus were taken into account to compute the area, as shown in Fig 1B. All gray levels below the threshold value were considered as background. The threshold was determined separately for the images corresponding to each fluorochrome, which were available as separate image files, for each series of images.

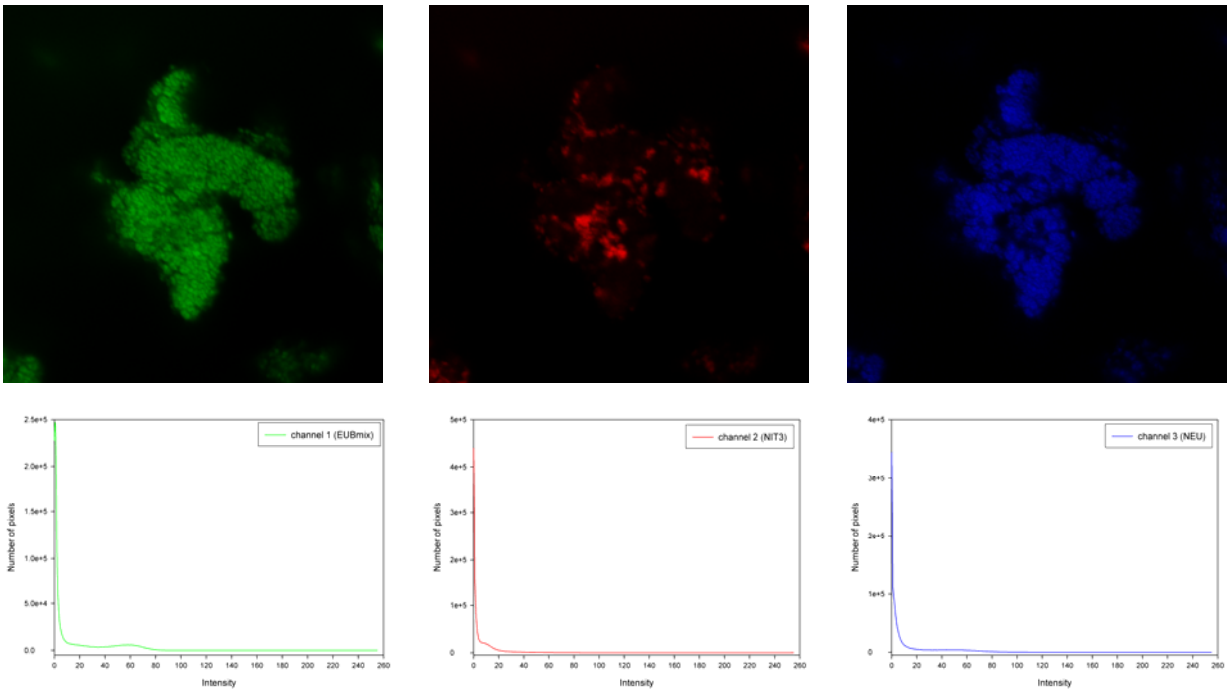

Fig 1A. Images obtained by CLSM corresponding to 3 different fluorochromes and the intensity histograms**.** The histograms show the number of pixels counted for each intensity between 0 and 256.

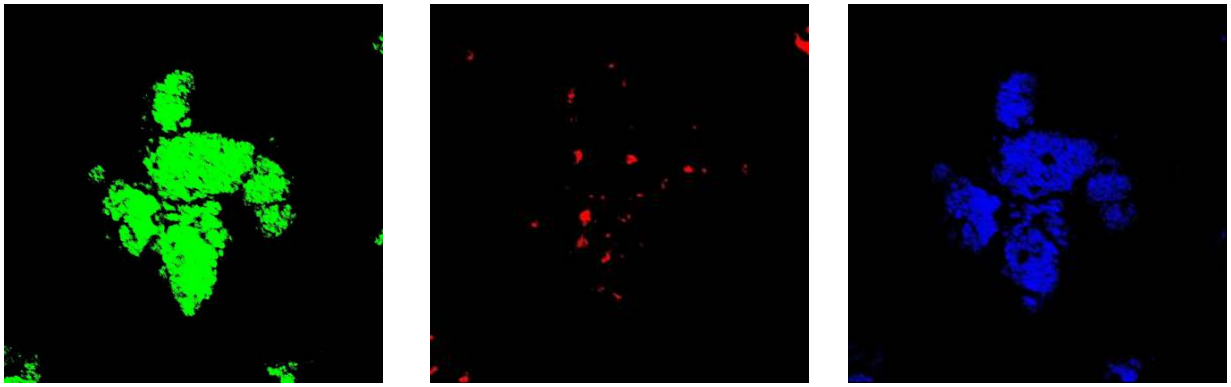

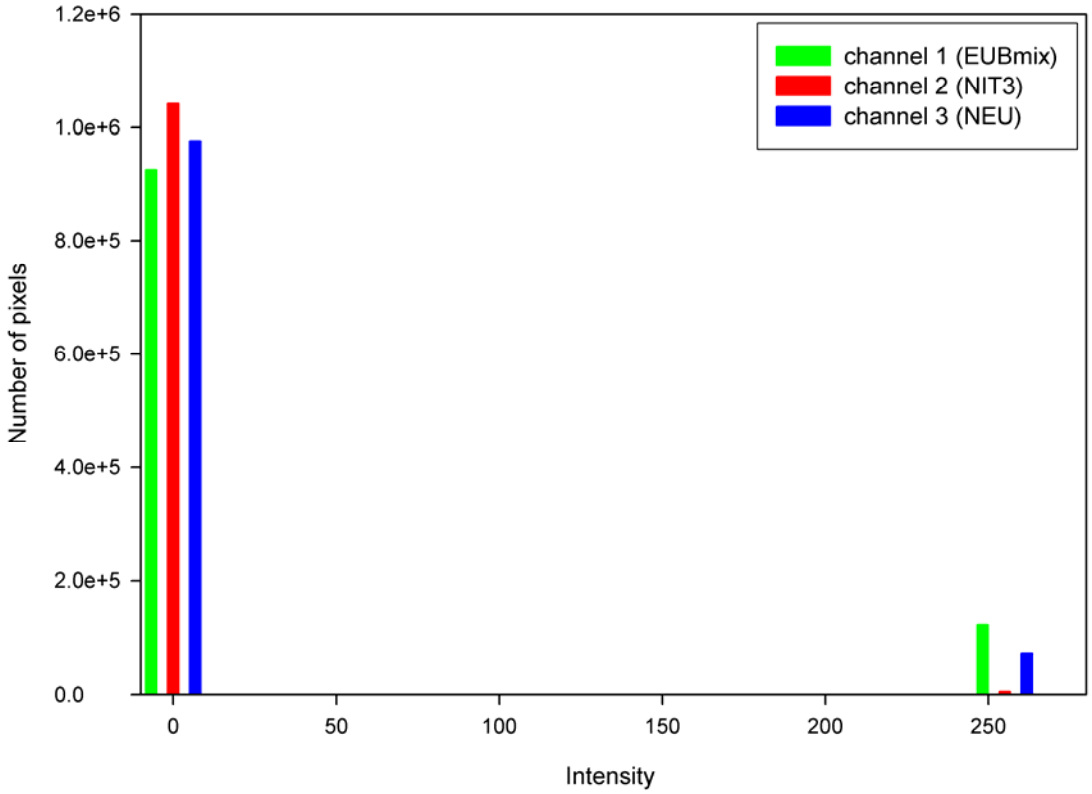

Fig 1B. Images obtained by CLSM corresponding to 3 different fluorochromes after thresholding. In the histograms it can be observed how all the pixels have been assigned an intensity of either 0 or 256.

Setting the threshold value allowed us to estimate the area covered by each one of the fluorochromes by counting the number of pixels that were assigned an intensity of 256, i.e. that have an intensity above the threshold. An histogram is presented (Fig. 1A, Fig. 1B), showing the number of pixels counted at each intensity.

The area of the binary images obtained after thresholding was estimated according to Eq. 1 and the total biovolume of each channel was obtained by applying an integration method as described by Hendrickx et. al., 2004.

$$X_i^j = A_{pixel} \cdot N_i^j \quad (1)$$

where:

- X_i: Area of each scanned position in a stack. The area of each section comprising a stack was determined separately and the data stored for integration.
- N_i^j: Number of pixels above the threshold level
- i: scanning position in the z direction starting (0<i<e)
- e: number of scanned positions within a stack

Numerical integration across the image stacks was applied to calculate the volume occupied by the cells stained by each one of the fluorochromes as described by Eq.2.

$$V_X^j = V_{X,e}^j = \frac{1}{2} \cdot (z_1 - z_0) \cdot X_0 + \sum_{i-1}^{e-2} \left(z_{(i+1)} - z_i\right) X_i + \frac{1}{2} \cdot \left(z_e - z_{(e-1)}\right) X_e \quad (2)$$

where:

- V_x^j: Total volume of a stack expressed in μm^3
- z: distance from the origin of the stack

- i: scanning position in the z direction starting (0<i<e)
- e: number of scanned positions within a stack
- X_i: Area of each scanned position

3. PRESENCE OF EXTRACELLULAR POLYMERIC SUBSTANCES (EPS) IN THE BIOFILM

Fresh samples were visualized with the CLSM after specific staining of cell nuclei and EPS. Syto13 or DAPI were used to target cell nuclei while a lectin probe tagged with a specific dye, (Con-A)-Texas Red, was used to target EPS. A full description of the protocols applied to perform these analyses was presented in TN 78.91. A number of 2-4 samples harvested from different packed-bed fractions were analyzed using this method.

EPS percentages estimated by CLSM image quantification ranged between 5% and 23% of the total sample biovolume. In Fig. 2 CLSM images obtained at different heights of the packed-bed are presented that confirm the presence of EPS in all the fractions of the packed-bed.

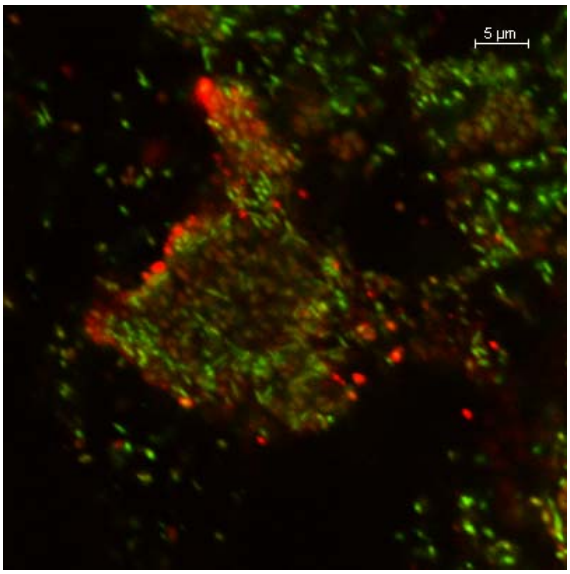

Fraction F0

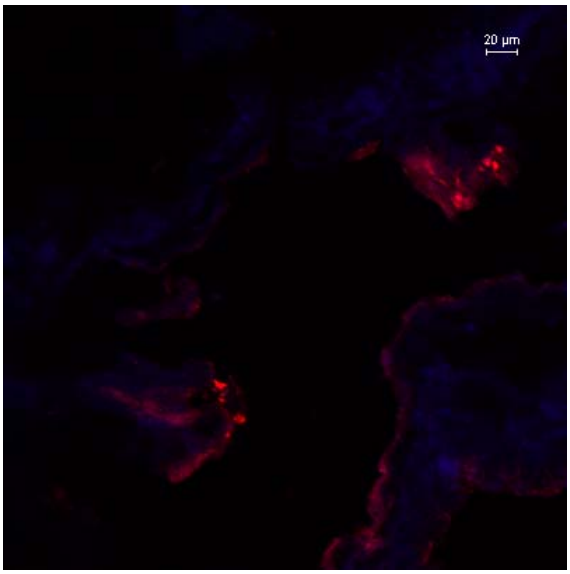

Fraction F2

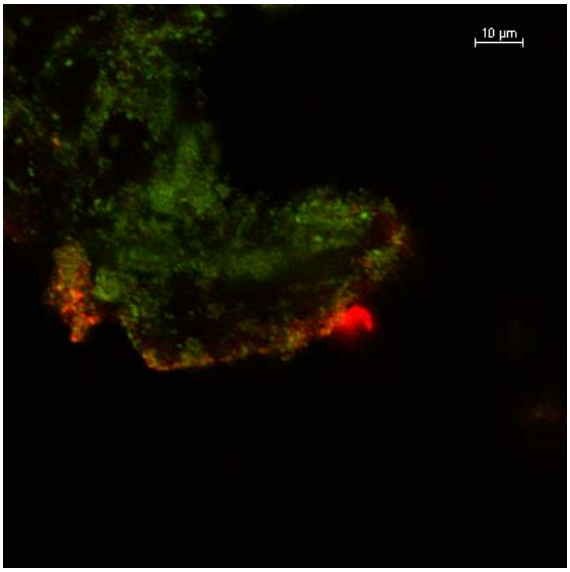

Fraction F4

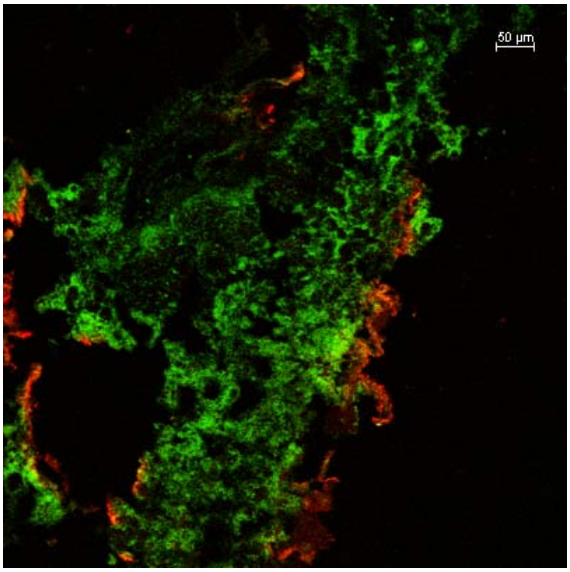

Fraction F5

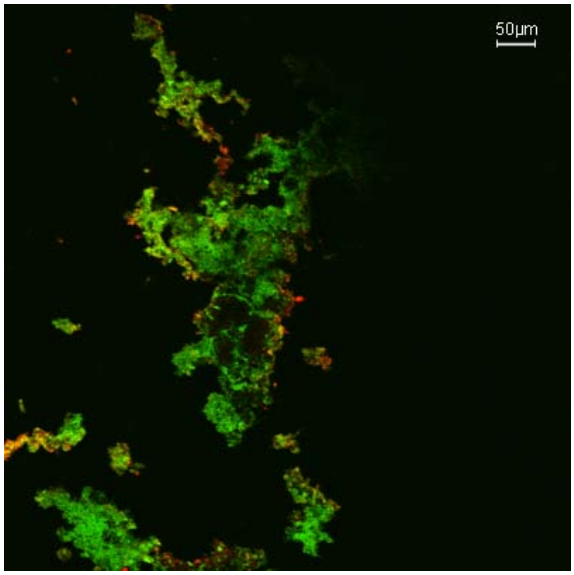

Fraction F7

Fig. 2: CLSM images corresponding to 5 different heights of the packed-bed: EPS (red, ConA-Texas Red) and cellular DNA (green, Syto13)

In Fig. 3 a slightly lower presence of EPS on the bottom part of the reactor can be observed. However, the percentages measured in the fractions F_2, F_4, F_5, and F_7 (heights comprised between 12 and 50 cm) did not point towards a clear trend of the EPS ratio along the packed-bed. An average value of 18% along the packed bed was estimated by quantification of the several image series obtained by CLSM.

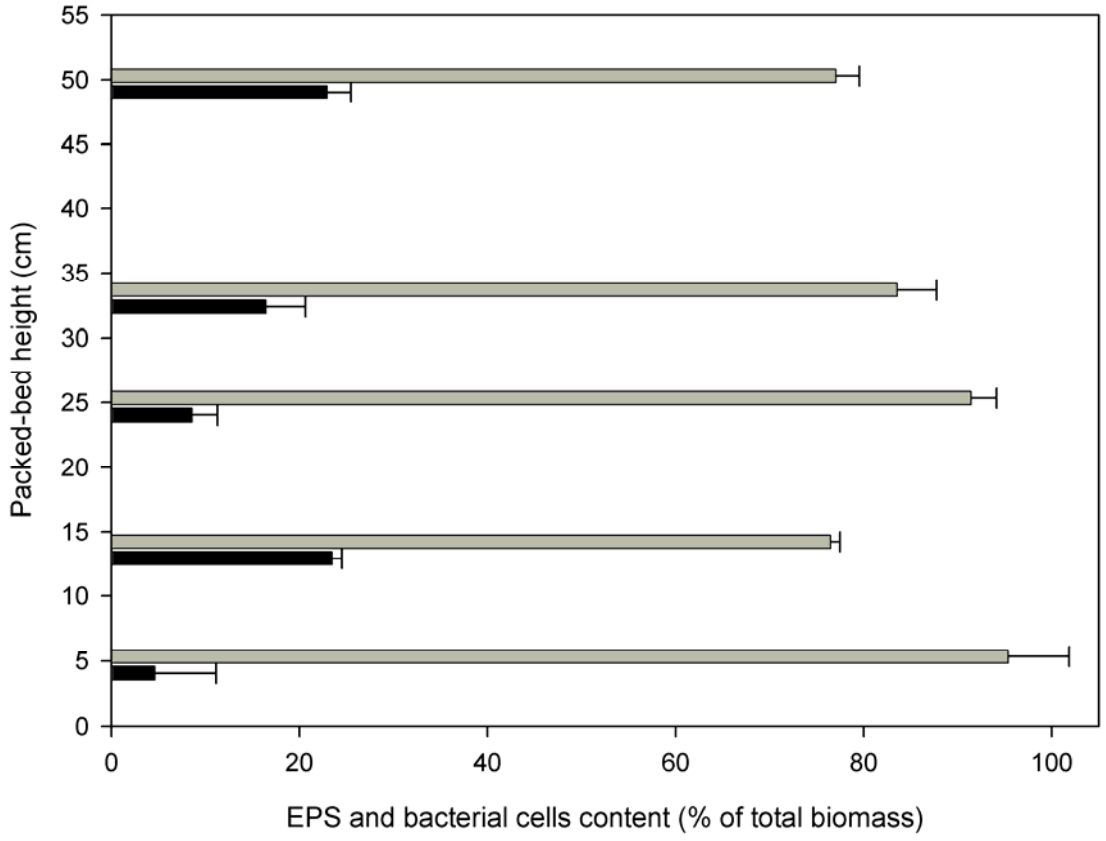

Fig. 3: EPS content (black bars) and bacterial cells content (grey bars) as obtained by analysis of CLSM images from samples belonging to different heights of the fixed-bed reactor.

4. BIOMASS CONCENTRATION PROFILE

A profile of total biomass concentration along the packed-bed was assessed by performing dry weight analysis of each of the eight fractions into which the contents of the reactor had been divided upon stop of the operation (Fig. 4). The porosity of the packed-bed was estimated by experimentally measuring the void fraction left by the Biostyr® beads with respect to the total reactor volume after the biomass had been separated from the beads. The porosity (0.39 mL void/ mL packed-bed) was used to estimate the total volumes of each one of the eight fractions, which were subsequently used to calculate the total biomass concentration to total fraction volume (Fig. 4)

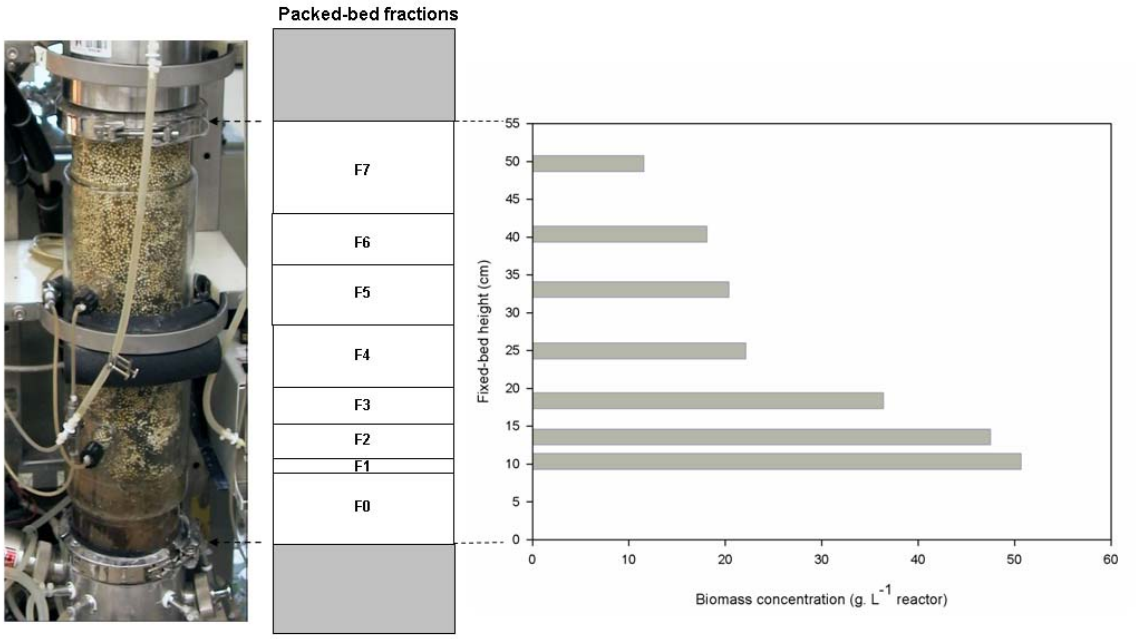

Fig. 4: Biomass concentration in the packed-bed as a function of the position along the vertical axis. A scheme with the fraction volumes in the packed-bed and a photograph of the reactor before dismantling is added to visualise the location of the different fractions. Reactor height is expressed as the average height of the packed-bed fraction from which the samples were obtained.

The estimated concentration profile was in agreement with previous observations (Pérez et al., 2004 & 2005) that pointed at a clear biomass accumulation near the feeding point of the reactor. This gradient is developed due to the fact that most characteristic times of the nitrification process are shorter than the mixing time in the bioreactor. Therefore, the mixing time is the controling parameter for biomass accumulation.

5. RELATIVE DISTRIBUTION OF *N. europaea* AND *N. winogradskyi* ALONG THE PACKED-BED

To estimate the degree of coverage of *N. europaea* and *N. winogradkyi* as dominant ammonia-oxidizing and nitrite-oxidizing species in the packed-bed, a number of samples were taken from a few parts throughout the packed-bed reactor and were subjected to FISH-CLSM analysis. The relative amounts of the targeted groups of bacterial species were calculated as the percentage of the total eubacterial biomass (EUBmix) for all probes, with only two exceptions in which the total EUBmix biovolume could not be estimated, as indicated in Table 5.

Probes targeting *Nitrosomonas* species (NEU) (Wagner et al., 1995) or *Nitrobacter* species (NIT3) (Wagner et al., 1996) were combined in samples F_0, F_4 and F_6 (Fig. 5).

In samples taken from F_0, the average amount of *Nitrosomonas* to total EUBmix biovolume (82±9%) and *Nitrobacter* to total EUBmix biovolume (10±2%) indicated a presence of other organisms of 15±9% of the total scanned volume (Table 5, Fig. 5D).

In addition the relative percentages of NEU and NIT3 to the total biovolume of nitrifying bacteria (NEU+NIT3) were calculated (Fig. 8), showing a clear decrease in the relative abundance of *Nitrosomonas* to total nitrifying biomass with increasing height. In fraction F0 the relative percentage of *Nitrosomonas* was 82±5% while in fraction F2 only 44% of the total NEU+NIT3 biovolume was found to be *Nitrosomonas*. In fraction F4 the relative amount of *Nitrosomonas* was of 11% as estimated by the same probe combination and in fraction F6 the relative amount of *Nitrosomonas* biovolume was of 5%. The decrease in the relative amount of *Nitrosomonas* along the vertical axis of the packed-bed can be qualitatively observed in the images presented in Fig.5, obtained at different reactor heights.

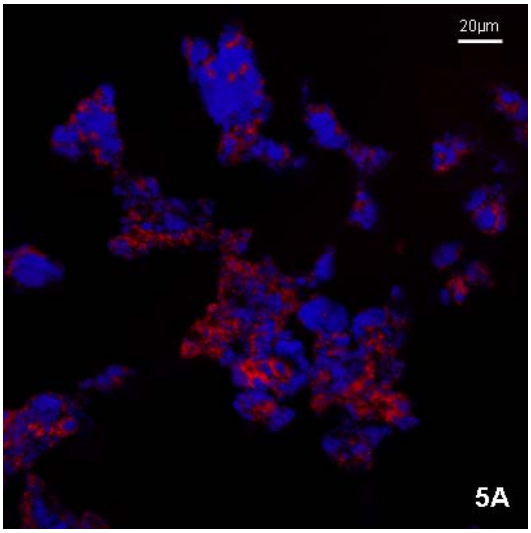

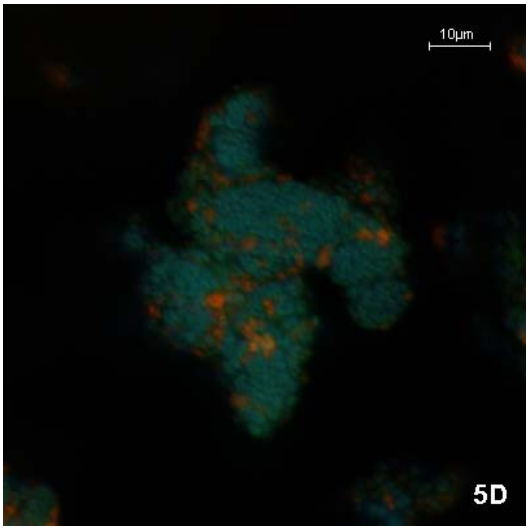

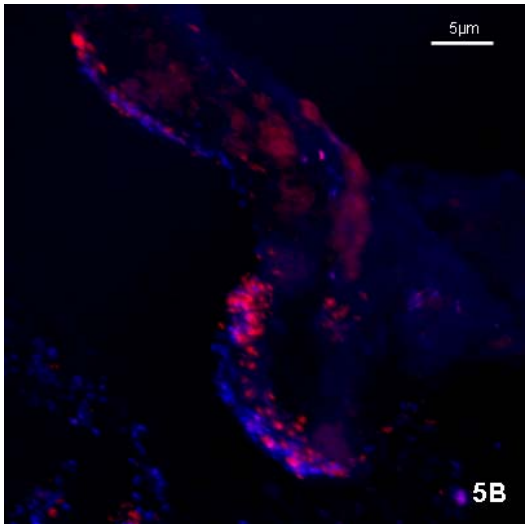

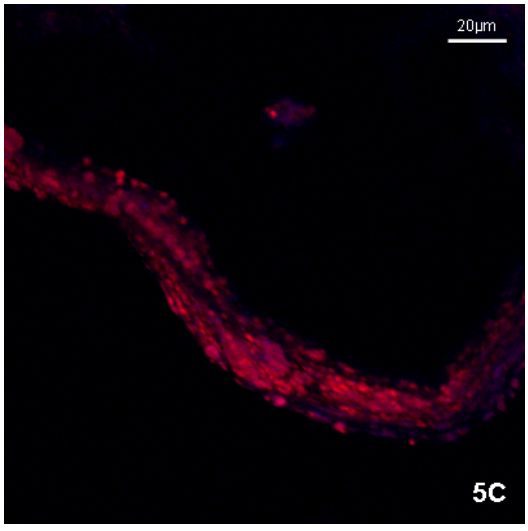

Fig.5: FISH images obtained at different heights of the packed-bed. A) Image depicting *Nitrosomonas* (NEU, blue) and *Nitrobacter* species (NIT3, red) in a sample taken from location F_0. B) Image depicting *Nitrosomonas* (NEU, blue) and *Nitrobacter* species (NIT3, red) in a sample taken from location F_4. C) Image depicting *Nitrosomonas* (NEU, blue) and *Nitrobacter* species (NIT3, red) in a sample taken from location F_6. D) Image depicting *Nitrosomonas* (NEU, blue), *Nitrobacter* species (NIT3, red) and total active bacteria (EUBmix, green) in a sample taken from fraction F0)

Qualitative analysis of FISH images using the GAM42 (*γ-Proteobacteria*) and CF319a/b (*Cytophaga-Flavobacterium* group) probes, targeting heterotrophic organisms most commonly spotted in nitrifying systems, showed in general very little presence of bacteria belonging to these taxa.

Using the GAM42 probe on samples from the fractions F_0, F_1 and F_4 revealed a presence of respectively 2.9%, 1.37% and 0.37% of cells belonging to the group of *γ-Proteobacteria* (Fig. 6A). The CF319a/b was applied in samples F_1 as well as in F_4, resulting in the detection of respectively 0.13% and 0.34% of the total scanned biomass, visualising bacterial cells belonging to the *Cytophaga-Flavobacterium* group (Fig. 6B).

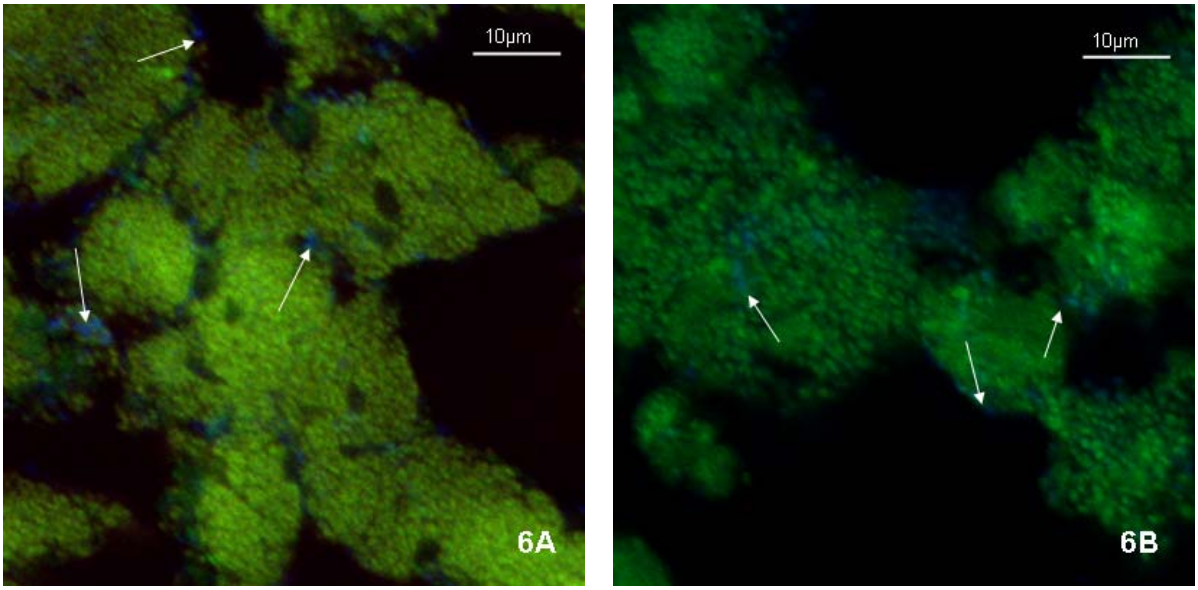

Fig. 6: FISH images at different heights of the packed-bed. A) Image depicting the presence of bacteria belonging to the γ-Proteobacteria (GAM42a, blue) in the biofilm (EUBmix, green) in a sample taken from location F_0. B) Image depicting bacteria belonging to the Cytophaga-flavobacterium group (CF319a/b, blue) in the biofilm (EUBmix, green) in a sample taken from location F4.

Hence, the contaminating organisms present in F_0 most probably belong to other taxa. To estimate the presence of other ammonia-oxidizing bacteria in the biofilm the *Nitrosomonas*-targeting Nse1472 probe was used in samples taken from F_0 and F_4 (Fig. 7) and were in good agreement with the biovolume in terms of percentage, detected using NEU (Table 5). This observation indicates that probably the most important ammonia-oxidizing organism remained *Nitrosomonas europaea* or a closely related species.

Although the FISH analysis could assess the dominance of the *Nitrosomonas europaea* and *Nitrobacter winogradskyi* in CIII, the absence of other AOB and NOB in CIII can only be confirmed with a more in depth community profiling study. However, this was at present beyond the scope of this study.

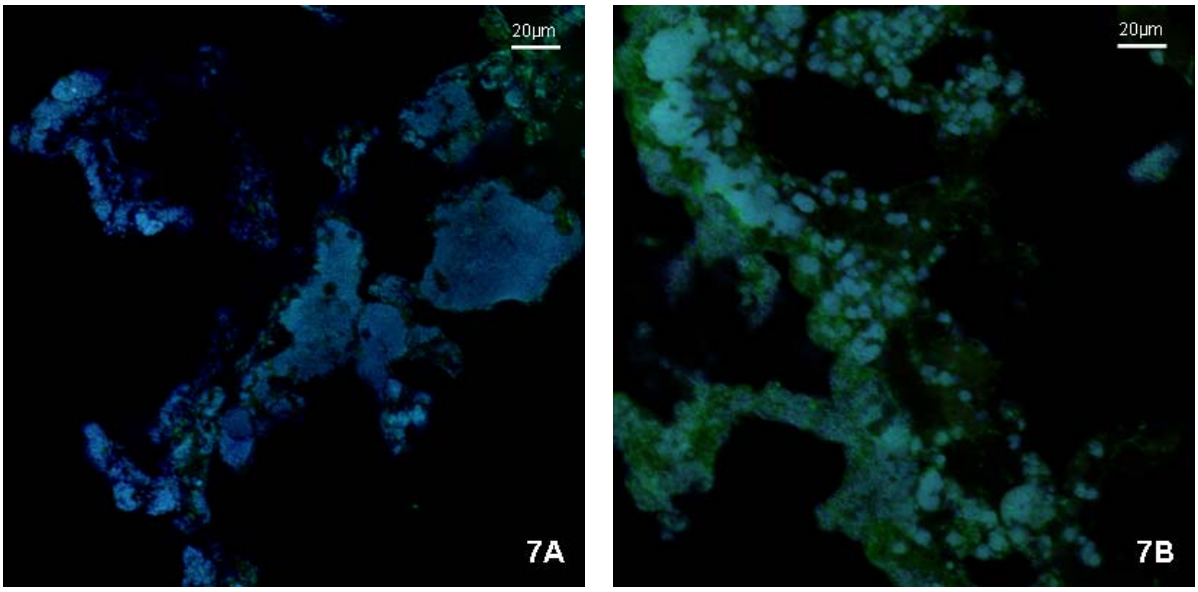

Fig. 7: FISH images obtained at different heights of the packed-bed. A) Image depicting *Nitrosomonas* (Nse1472, blue) in the biofilm (EUBmix, green) in a sample taken from location F_0. B) Image depicting *Nitrosomonas* (Nse1472, blue) in the biofilm (green) in a sample taken from location F_4.

Table 5 - Relative abundance of *N. europaea* and *N. winogradskyi* along the vertical axis of the packed-bed as depicted by FISH (percentage related to total biovolume as estimated by EUB338mix except † for which the percentages are referred to total NEU+NIT3 biovolume). (n) indicates the number of samples used to obtain the average value for each fraction. Scanned biofilm volume was taken into account in the calculation of average FISH percentages.

Fraction	**Height (cm)**	***N. europaea*** Abundance (%)	***N. winogradskyi*** Abundance (%)
F0	4.7	*NEU:* 82 ±9 (3) *Nse1472:* 81 (1)	*NIT3:* 10±2 (2)
F1	10.4	-	*ALF1B:* 17 (1)
†F2	13.6	*NEU:* 44 (1)	*NIT3:* 56 (1)
F3	18.4	*Nse1472:* 44 (1)	-
F4	25.0	*NEU:* 11 (1) *Nse1472:* 34 ±23 (2)	*NIT3:* 98 (1)
F5	33.0	-	*ALF1b:*60±13 (2)
†F6	40.4	*NEU:* 5 (1)	*NIT3:* 95 (1)
F7	49.7	-	-

The efficiency of FISH is known to be strongly influenced by numerous factors: (i) the choice of probes and fluorochromes; (ii) the hybridisation temperature, (iii) auto-fluorescence of some microorganisms or components of the sample matrix that might lead to false-positive or false-negative results (Dorigo *et al.*, 2005).

Probes with different degrees of specificity were selected that ranged from the very specific up to the very general (as widely addressed in TN 78.91). Nitrifying bacteria were thus targeted in a hierarchical cascade, and in addition some probes specific to groups other than those of *Nitrosomonas* and *Nitrobacter* were used in an attempt to obtain as much information as possible from the biofilm analysis.

The quantification of FISH images was based on an area quantification method that unavoidably has a certain error. The error was minimised by combining the area estimations obtained with several samples when available, and the area estimated for each sample and presented in Table 5 is the result of averaging the estimations obtained

with different samples and weighing the obtained value with the total scanned volume of biofilm in each sample.

In Fig. 8 the proportions of *Nitrosomonas* to total biofilm volume (Fig. 8A) and *Nitrobacter* to total biofilm volume (Fig. 8B) are presented as a function of packed-bed height. A decrease in the *N. europaea* proportion with increasing reactor height can be observed which is in good correlation with the predictions of the mathematical model as described in Pérez *et al*., 2004.

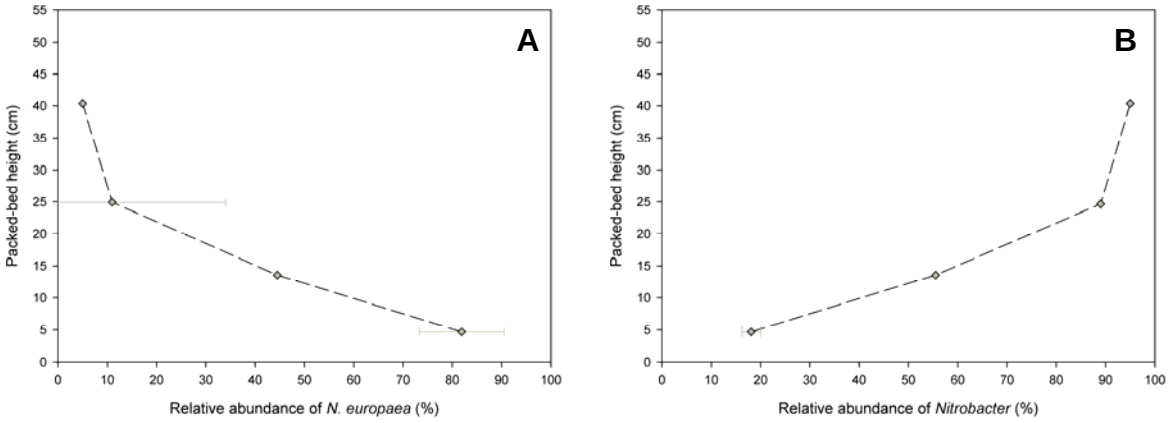

Fig. 8: Relative distribution of N. europaea and N. winogradskyi along the packed-bed as depicted by FISH-CLSM analysis. A) Ratio between the amount of *N. europaea* and the total NEU+NIT3 biovolume. B) Ratio between the amount the amount of *N. winogradskyi* and the total NEU+NIT3 biovolume.

6. CONCLUSIONS

- The nitrifying biofilm from compartment III pilot reactor was analyzed by means of a molecular-based technique that made it possible to obtain some relevant information regarding the biomass distribution along in the pilot reactor of compartment III after 4.8 years of continuous operation.
- The increasing biomass concentration along the packed-bed was experimentally quantified confirming the observations of previous periods of operation for this reactor.
- FISH analysis coupled with CLSM observation and subsequent quantification allowed us to experimentally assess the segregation of the two bacterial species *N. europaea* and *N. winogradskyi* along the packed-bed that had already been predicted by the mathematical model. The proportion of *N. europaea* shows a general trend to decrease with height in the packed-bed while the proportion of *N. winogradskyi* in the biofilm was found to increase with increasing height.
- After 4.8 years of continuous operation *N. europaea* and *N. winogradskyi* are still the dominant strains in compartment III, which is important to assess the long term stability of the nitrifying compartment of the MELiSSA.
- The characterisation of the nitrifying biofilm of the MELiSSA compartment III has provided experimental evidence on the relative distribution of the two bacterial strains involved in the nitrification process, increasing the knowledge on the system and thus being of great importance to control and improve the reactor performance.

7. LIST OF ABBREVIATIONS AND ACRONYMS

AOB	Ammonia Oxidising bacteria
CIII	MELiSSA compartment III
CLSM	Confocal Laser Scanning Microscopy
EPS	Extracellular Polymeric Substances
FISH	Fluorescent *In Situ* Hybridization
NOB	Nitrite Oxidising bacteria
RTD	Residence Time Distribution
N. europaea	*Nitrosomonas europaea*
N. winogradskyi	*Nitrobacter winogradskyi*

8. REFERENCES

Amann R., Krumholz L. and Stahl D.A. (1990) Fluorescent oligonucleotide probing of whole cells for determinative, phylogenetic, and environmental studies in microbiology. Journal of Bacteriology: 172: 762-770.

Amann, R.I. (1995) In situ identification of micro-organisms by whole cell hybridization with rRNA-targeted nucleic acid probes. p. 1-15. In Akkermann, ADC, van Elsas, J.D. and de Bruijin F.J. (ed.) Molecular Microbiology Ecology Manual. Kluwer Academic Publishers, Dordrecht

Aoi,, Y; Miyoshi, T.; Okamoto, T; Tsuneda, S; Hirata, A.; Kitayama, A. and Nagamune, T. (2000) Microbial ecology of nitrifying bacteria in wastewater treatment process examined by fluorescence *in situ* hybridization. Journal of Bioscience and Bioengineering; 90 (3):234-240.

Aoi, Y.(2002). *In Situ* identification of microorganisms in biofilm communities. Journal of Bioscience and Bioengineering; 94, 6: 552-556.

Burell P.C., Keller J. and Blackall L.L. (1998) Microbiology of a nitrite-oxidizing bioreactor. Applied Environmental Microbiology; 64 (5): 1878-1883.

Caldwell, D.E., D.R. Korber and J.R. Lawrence. 1992. Confocal laser scanning microscopy and digital image analysis in microbial ecology. Adv. Microbial Ecol. 12:1-67.

Chalfie, M., Y. Tu, G. Euskirchen, W.W. Ward, and D.C. Prasher. 1994. Green fluorescent protein as a marker for gene expression. Science 263:802-805.

Daims H, Nielsen P, Nielsen JL, Juretschko S and Wagner M. (2000) Novel *Nitrospira*-like bacteria as dominant nitrite oxidizers in biofilms from wastewater treatment plants: diversity and in situ physiology.Water Science and Technology; 41(4-5):85-90.

Daims H, Nielsen JL, Nielsen PH, Schleifer KH and Wagner M. (2001). In situ characterization of Nitrospira-like nitrite oxidizing bacteria active in wastewater treatment plants. Applied and Environmental Microbiology 67, 5273-5284.

Geisenberger, O., A. Ammendola, B.B. Christensen, S. Molin, K.-H. Schleiffer, and L. Eberl. 1999. Monitoring the conjugal transfer of plasmid RP4 in activated sludge and in situ identification of the transconjugants. FEMS Microbiol. Lett. 174:9-17.

Gòdia, F.; Albiol, J.; Montesinos, J.L.; Pérez, J.; Creus, N.; Cabello, F; Mengual, X.; Montràs, A.; Lasseur, Ch. (2002) MELISSA: a loop of interconnected bioreactors to develop life support in Space. Journal of Biotechnology 99: 319-330

Hartmann, A., J.R. Lawrence, B. Assmus, and M. Schloter. 1998. Detection of microbes by laser confocal microscopy. Mol. Microbial Ecol. Manual 4:1-34.

Hendrickx, L., M. Hausner, and S. Wuertz. 2000. In situ monitoring of natural genetic transformation of Acinetobacter calcoaceticus BD413 in monoculture biofilms. Water Sci. Technol. 41:155-158.

Hendrickx, L. and Wuertz, S. (2004) Investigating *in situ* natural genetic transformation of *Acinetobacter* sp. BD413 in biofilms with confocal laser scanning microscopy. Genetic Engineering 26: 159-173

Hugenholtz P., Tyson G.W. and Blackall L. (2001). Design and evaluation of 16S rRNA-targeted oligonucleótido probess for fluorescence *in situ* hybridization. Methods in Molecular Biology, 176: 29-41

Juretschko s, Timmermann G, Shmid M, Schleifer KH, Pommerening-Röser, Koops HP and Wagner M. (1998) Combined molecular and concentional analyses of nitrifying bacterium in activated sludge: *Nitrosococcus mobilis* and *Nitrospira*-like bacteria as dominant populations. Applied Environmental Microbiology 64(8):3042-3051

Kindaichi T., Kawano Y., Ito T., Satoh H. and Okabe S. (2006) Population dynamics and *in situ* kinetics of nitrifying bacteria in autotrophic nitrifying biofilms as determined by Real-Time Quantitative PCR. Biotechnol. Bioeng. 94: 1111-1121.

Kuehn, M., M. Hausner, H.-J. Bungartz, M. Wagner, P.A. Wilderer, and S. Wuertz. 1998. Automated confocal laser scanning microscopy and semiautomated image processing for analysis of biofilms. Appl. Environ. Microbiol. 64:4115-4127.

Lawrence, J.R.; Neu, T.R. and Swerhone, G.D.W. (1998). Application of multiple parameter imaging for the quantification of algal, bacterial and exopolymer components of microbial biofilms. Journal of microbiological methods 32: 253-261

Loy A., Horn M. and Wagner M. (2003) ProbeBase: an online resource for rRNA targeted oligonucleotid probes. Nucleic Acids Research 31: 514-516.

Lydmark P., Lind M., Sörensson F. and Hermansson M. (2006) Vertical distribution of nitrifying populations in bacterial biofilms from a full-scale nitrifying trickling filter. Environm. Microbiol. 8:2036-2049.

Manz W, Amann R, Ludwig W, Wagner M, and Schleifer KH. (1992) Phylogenetic oligonucleotide probes for the major subclasses of Proteobacteria: problems and solutions. Systematic and Applied Microbiology 15:593-600.

Manz W, Amann R, Ludwig W, Vancanneyt M and Schleifer KH. (1996) Application of a suite of 16S r-RNA-specific oligonucleotide probes designed to investigate bacteria of the phylum *Cytophaga-Flavobacter-Bacteroides* in the natural environment. Microbiology 142: 1097-1106.

Mobarry B.K., Wagner M., Urbain V., Rittmann B. and Stahl, D.A. (1996) Phylogenetic probes for analyzing abundance and spatial organization of nitrifying bacteria. Applied Environmental Microbiology 62:2156-2162.

Montràs A., Hendrickx L. and Pérez J. (2005). Nitrifying biofilms in biological life support systems for Space missions. 3rd International Workshop on Space Microbiology. Mol, Belgium 22nd-25th May 2005. Poster.

Nogueira, R.; Melo, L.F.; Purkhold, U; Wuertz, S and Wagner, M. (2002) Nitrifying and heterotrophic population dynamics in biofilm reactors: effects of hydraulic retention time and the presence of organic carbon. Water Research 36: 469-481.

Okabe S., Naitoh H., Satoh H. and Watanabe Y. (2002) Structure and function of nitrifying biofilms as determined by molecular techniques and the use of microelectrodes. Water Sci Tech 46: 233-241.

Okabe, S. ; Satoh, H. and Watanabe, Y. (1999) In situ analysis of nitrifying biofilms as determined by in situ hybridization and the use of microelectrodes. Applied Environmental Microbiology 65: 3182-3196.

Pérez, J.; Montesinos, J.L.; Gòdia, F. (1996). Nitrifying Compartment Studies. Starting of the nitrifying reactor. Technical Note 25.310. ESTEC CONTRACT 11549/95/NL/FG.

Pérez, J.; Montesinos, J.L.; Gòdia, F. (1996). Nitrifying Compartment Studies. Starting of the nitrifying reactor. Technical Note 25.320. ESTEC CONTRACT 11549/95/NL/FG.

Pérez, J.; Montesinos, J.L.; Gòdia, F. (1996). Nitrifying Compartment Studies. Starting of the nitrifying reactor. Technical Note 25.330 . ESTEC CONTRACT 11549/95/NL/FG.

Pérez, J.; Montesinos, J.L. and Gòdia, F.; (1998).Operation of the Nitrifying Pilot Reactor. Technical Note 37.420. ESTEC CONTRACT 11549/95/NL/FG.

Pérez, J.; Montesinos, J.L.; Albiol, J. and Gòdia, F. (2004) Nitrification by immobilized cells in a micro-ecological life support system using packed-bed bioreactors. Journal of Chemical Technology and Biotechnology 79: 742-754

Pérez, J.; Poughon, L.; Dussap, C.-G.; Montesinos, J.L. and Gòdia, F. (2005) Dynamics and steady state operation of a nitrifying fixed bed biofilm reactor: mathematical model based description. Process Biochemistry 2005; 40: 2359-2369

Persson, F.; Wik, T; Sörensson, F. and Hermansson, M. (2002) Distribution and activity of ammonia oxidizing bacteria in a large full-scale trickling filter. Water Research 36: 1439-1448.

Pommerening-Röser A., Rath G. and Koops H.P. (1996) Phylogenetic diversity within the genus *Nitrosomonas*. Systematic and Applied Microbiology 19(3): 344-351.

Sakano, Y.; Pickering, K.D.; Strom, P.F. and Kerkhof, L.J. (2002) Spatial distribution of total, ammonia-oxidizing, and denitrifying bacteria in biological wastewater treatment reactors for bioregenerative life support. Applied Environmental Microbiology 68: 2285-2293.

Schramm A., De Beer D., Gieseke A. and Amann R. (2000) Microenvironments and distribution of nitrifying bacteria in a membrane-bound biofilm 2: 680-686.

Schramm, A. (2003) In situ analysis of structure and activity of the nitrifying community in biofilms, aggregates and sediments. Geomicrobiological Journal 20, 313-333.

Strathmann, M.; Wingender, J. and Flemming, H. (2002) Application of fluorescently labelled lectins for the visualisation and biochemical characterization of polysaccharides in biofilms of *Pseudomonas aeruginosa.* Journal of microbiological methods 50:237-248.

Thurnheer, T.; Gmür, R. and Guggenheim, B. (2004) Multiplex FISH analysis of a six-species bacterial biofilm. Journal of Microbiological Methods 56: 37-47.

Wagner M., Rath G., Amann R.I., Koops H.P. and Schleifer K.H. (1995) In situ identification of ammonia-oxidizing bacteria. Systematic and Applied Microbiology 18 (2) 251-264.

Wagner M., Rath G., Koops H.P., Flood J. and Amann R. (1996) In situ analysis of nitrifying bacteria in sewage treatment plants. Water Science and Technology 34 (1-2):237-244.

Wolfaardt, G.M.; Lawrence, J.R.; Robarts, R.D. and Caldwell, D.E. (1998). In situ characterisation of biofilm exopolymers involved in the accumulation of chlorinated organics. Microbial Ecology 35: 213-223

9. ANNEX

All the CLSM raw images that were obtained from the FISH analysis as well as the images obtained from the analysis of fresh samples and used for the subsequent quantification, can be found in the DVD-R enclosed with the Technical Note document.

10. COMMENTS

TN 78.92: Biofilm studies in compartment III pilot reactor: Analysis and discussion of the results				
Comment Nr.	**Page/Paragraph**	**Description of comment**	**Answer**	**Comment status**
1	General	Could you present all raw results obtained for all analyses in Annex for the sake of tracability? The TN should be more detailed than for a publication (i.e. presents all results).	All the images that were obtained from the FISH analysis and from the analysis of fresh samples have been included as annex information in digital format (a DVD has been enclosed). The images that were not relevant for the discussion have been omitted from the printed document to avoid unnecessary information but have been included in the annex.	
2	2. Quantification of CLSM images	On which criteria did you define the appropriate intensity threshold for each fluorochrome?	The threshold was set using the tools provided by the LEICA image analysis software, which allowed us to work with images from the different channels simultaneously. The background signal that was observed in all the channels and thus could not be attributed to each fluorochrome was set as the threshold. This procedure was repeated for each sample.	
3	2. Quantification of CLSM images	Could you justify that the fluorochrome selected have the same performances i.e. the level of intensity/cell density is similar for each fluorochrome selected?	It is not possible to confirm that the intensities are similar for the different fluorochromes, or for the different samples, as the intensity also depends on the good performance of the hybridisation procedure. However, due to the quantification procedure used it is not necessary to have similar intensities in each channel: the fact that a threshold is set for each of the channels in every sample allows us to correlate this resulting "relative intensity" in each channel (the result of irradiating each fluorochrome with the correct wavelength by means of a laser) with the number of positive pixels and consequently with an area by knowing the pixel size, which is set up in advance. The areas with a positive signal (above the threshold) for each fluorochrome are computed for every layer and integratio finally leads to a biovolume occupied by each targeted species. It is the area computed from the relative intensities (related to the threshold) and not the absolute value of the intensity that leads to the quantification results.	
4	3. Presence of EPS in the biofilm	Could you present all results related to the quantification of EPS versus cell nuclei or justify the omissions? E.g. results with ConA and DAPI is missing for fraction 0.	Only a few images that were representative of the obtained results were presented to avoid duplicate information. As the results obtained with DAPI and Syto 13 staining proved to be very similar (both are nucleic acid stains and thus specific to cell nuclei), only a few images have been presented as an example of the raw data from which the quantification was performed. The results obtained from quantification of samples at different fractions of the packed bed have been included in Fig. 3 and all the available raw images used to attain these results have now been included as an annex (enclosed DVD).	
5	3. Presence of EPS in the biofilm	Would you make clear the characteristics of Syto 13 and DAPI for the sake of clarity?	Both DAPI and Syto13 are nucleic acid stains that have different excitation and emission wavelengths. The information provided by both stains is similar, but the use of either one will depend on the application (e.g. DAPI is sometimes used as a counterstain to be used in combination with FITC fluorochrome, while Syto 13 can not be used for this application due to the similar emission wavelength). Both stains proved a good performance when used in fresh samples in combination with ConA-Texas Red to stain microbial EPS.	
6	3. Presence of EPS in the biofilm	Could you determine to proportion of live/dead cells along the column or would you have any preliminary results?	It was not possible to estimate the proportion of live/dead cells in each fraction due to a time constraint.	
7	Page 11	Could you elaborate more on any expectation for an EPS ratio trend along the packed-bed?	The data obtained from quantification of the images obtained at different heights did not show a clear trend along the packed bed. The presence of EPS depends on several factors and it is difficult to hypothesize and elaborate on possible trends.	

8	Page 11	Could you discuss the 18% value in relation with the existing model?	The existing model allowed the prediction of some trends regarding the concentration and thus the relative distribution of the two bacterial species *N.europaea* and *N.winogradkyi* along the packed bed. The mathematical model cannot be used to make any predictions regarding the presence of EPS in the packed bed, as the processes related to the production of EPS by the cells were not implemented in the mathematical model.	
9	Page 11, Figure 3	Error - bar is missing	This issue has been corrected in Fig. 2 (page10). In addition the legend in Fig. 2 has been modified to clarify what can be seen in the images.	
10	Page 12	Could you describe the method applied to assess the porosity of the packed-bed?	After the operation of the reactor was stopped and the biofilm samples taken, the remaining biofilm was detached from the substratum. The biomass was freeze-dried and the Biostyr beads were used to estimate the porosity of the bed. The beads were put in a 1L test tube and water was added to fill the voids left by the Biostyr beads. The amount of water in relation to the total volume occupied by the packed substratum allowed us to estimate the porosity.	
11	Page 13	Could you give value on nitrification process speed versus mixing time?	We cannot give a value for the nitrification process speed, however, what we intended to point out in this paragraph is the fact that most characteristic times involved in the nitrification process are higher than the mixing time, leading to a preferent growth of biomass on the lower sections of the packed bed. This trend had already been predicted by the mathematical model and the data presented in this Technical Note provide experimental evidence.	
12	Page 13	Can we correlate the data obtained with nitrification efficiency value along the packed-bed?	There is no availability of experimental data of the liquid phase composition at different bed heights, only the overall efficiency of the nitrification process at the time the reactor operation was stopped could be measured.Therefore it is not possible to correlate the relative distribution of *N. europaea* and *N. winogradskyi* along the packed bed with any possible nitrogen concentration gradients along the packed bed.	
13	Page 14	Could you make clear for which 2 fractions the total EUBmix biovolume could not be estimated and why?	The two fractions whose EUBmix biovolume could not be estimated are fractions F2 and F6, as indicated in the legend in ***table 5, page 18*** .The EUBmix probes where tagged with the FITC fluorochrome, which suffered severe photobleaching. Although the intensity of the laser beam was kept low, in some of the samples the phenomenon of photobleaching could not be avoided and the emitted intensity was too low to allow quantification of the EUBmix area.	
14	Page 14	The probe partitioning per fraction in Table 5 are different than the sample/probe combination presented in Table 10 TN78.91? Could you harmonize please?	The information contained in Table 10 TN78.91 was simply a raw list of the probe combinations that we intended to perform and the combinations that were successfullycarried out. In Table 5 TN78.92 we intend to summarize the processed data, and hence the difference in the format. In Table 5 the quantification data obtained from the different probe combinations have been listed in two different categories, depending on whether they provide information on the amount of *N. europaea* or *N. winogradsky* . We think it is important to list the processed data in such a way that they provide us with the information as required by the discussion and for this reason we would like to suggest to keep the format as it is, otherwise we think it could become confusing for the discussion.	

14	Page 14	The probe partitioning per fraction in Table 5 are different than the sample/probe combination presented in Table 10 TN78.91? Could you harmonize please?	The information contained in Table 10 TN78.91 was simply a raw list of the probe combinations that we intended to perform and the combinations that were successfullycarried out. In Table 5 TN78.92 we intend to summarize the processed data, and hence the difference in the format. In Table 5 the quantification data obtained from the different probe combinations have been listed in two different categories, depending on whether they provide information on the amount of *N. europaea* or *N. winogradsky*. We think it is important to list the processed data in such a way that they provide us with the information as required by the discussion and for this reason we would like to suggest to keep the format as it is, otherwise we think it could become confusing for the discussion.	
15	Page 14	Could you provide detailed results concerning the presence of other organisms and their fraction 15%? How did you determine the 15% fraction?	The average value of 15% was determined by computing the total biovolume corresponding to the EUBmix probe that did not give a positive signal for either the *Nitrosomonas* or the *Nitrobacter* specific probes, but was positive to EUBmix. This value was obtained as an average from different samples. Due to a time constraint it was not possible to perform an exhaustive FISH analysis with probes that targeted any possible contaminants in samples from every fraction of the packed bed, so it is not possible to elaborate more on any differences regarding the presence and identity of the contaminants. However, we think the results of this study are sufficient to conclude that the bacterial community was still dominated by the two original strains *N. europaea* and *N. winogradskyi*, which is of great importance to guarantee the stability of the compartment.	
16	Page 15	In line with Comment 1, could you present images obtained with EUB probes combined with NIT3/NEU probes?	A new image has been added in Fig 5 (5D) in which the EUBmix stained area can be observed against the NEU (*N. europaea*) and NIT3 (*Nitrobacter species*) areas to illustrate the high proportion of *N. europaea* and *N. winogradskyi* present in the reactor.	
17	Page 16	Could you discuss the distribution of the contaminants among *Nitrosomonas* and *Nitrobacter* and along the packed bed?	The FISH analysis of the samples obtained from compartment III was oriented at assessing the predominance of *Nitrosomonas* and *Nitrobacter* after long term operation. Due to a time constraint regarding the availability of the CLSM facility, and due to the fact that all samples were obtained simultaneously (after stopping the reactor) it was not possible to perform an exhaustive search for other species in every fraction that allowed us to identify and quantify the possible contaminants. However, the results obtained allowed us to conclude that a very high percentage of the bacterial population present in the packed bed of compartment III belonged to the two original strains: *Nitrosomonas* and *Nitrobacter*. For this reason, the discussion in this Technical Note has been focused on the fact that the bacterial population was hardly altered after more than 4 years of continuous operation, with only a minor presence of other microorganisms. Further analyses would be required to identify and quantify the possible contaminants.	
18	Page 16, Figure 6	To which fraction of the column corresponds image B) (F1 or F4)?	Image 6B corresponds to a sample taken from location F4 in the packed bed. This issue has been corrected in the legend of Fig. 6 (p. 16)	

19	Page 20, Conclusions	Could you provide some conclusions, perspectives regarding the following points: - rationales for distribution of *N. winogradskyi* and *N. europea* along the packed-bed - repartition of N. winogradskyi and N. europea per fraction - significance of contamination and perspective for maintenance of axenicity - necessity to confirm the presence of the initially introduced strains and contaminants - correlation of present results with existing model - interest of a better characterization of the Melissa nitrifying biofilm - 3D images of the 10 um biofilm intervals	**repartition of *N. europaea* and *N. winogradskyi* along the packed bed and per fraction**: the contents of the packed bed were divided into a limited number of fractions (8), which proved to be enough to see the possible trends in the proportion of both species as shown in Fig. 8. As stated in the conclusions the results of the FISH analysis reveal a trend of the *N. europaea* proportion the decrease with increasing height leading to the profile of Fig. 8. Observing the profile within a fraction would be equivalent to dividing the packed bed content into a higher number of fractions, thus providing more data to be included in Fig 8, but the profile would be expected to be very similar. ***Significance of contamination and perspective for maintenance of axenicity***: the fact that the reactor was operated for almost 5 years without any major contamination is a good perspective for long term stability. To improve the long term operation of the reactor several improvements have already been approved and will be implemented in compartment III (TN 78.61). In the conclusions the following paragraph has been added to make it clear that the trend showed by the FISH results is in agreement with the model predictions: "*FISH analysis coupled with CLSM observation and subsequent quantification allowed us to experimentally assess the segregation of the two bacterial species N. europaea and N. winogradskyi along the packed-bed that had already been predicted by the mathematical model.*" ***Interest of better characterisation of the MELiSSA nitrifying biofilm:*** the confirmation of the results of a segregation of the two bacterial communities are of great importance as they contribute to increase the knowledge on the system and can therefore help improve the operation of the reactor. A paragraph has been added in the conclusions stating the importance of this characterisation: "*The characterisation of the nitrifying biofilm of the MELiSSA compartment III has provided experimental evidence on the relative distribution of the two bacterial strains involved in the nitrification process, increasing the knowledge on the system performance and thus being of great importance to control and improve the reactor performance.*" Unfortunately we do not have any images where the 3D biofilm structure can be observed, the biovolumes were numerically quantified but no images were generated.	